Clinical study of quantitative diagnosis of early cervical cancer based on the classification of acetowhitening kinetics

Tao Wu[*]
Hong Kong University of Science and Technology
Department of Electronic and Computer Engineering
Clear Water Bay
Kowloon, Hong Kong, China

Tak-Hong Cheung
So-Fan Yim
Chinese University of Hong Kong
Prince of Wales Hospital
Department of Obstetrics and Gynecology
Hong Kong, China

Jianan Y. Qu[†]
Hong Kong University of Science and Technology
Department of Electronic and Computer Engineering
Clear Water Bay
Kowloon, Hong Kong, China

Abstract. A quantitative colposcopic imaging system for the diagnosis of early cervical cancer is evaluated in a clinical study. This imaging technology based on 3-D active stereo vision and motion tracking extracts diagnostic information from the kinetics of acetowhitening process measured from the cervix of human subjects *in vivo*. Acetowhitening kinetics measured from 137 cervical sites of 57 subjects are analyzed and classified using multivariate statistical algorithms. Cross-validation methods are used to evaluate the performance of the diagnostic algorithms. The results show that an algorithm for screening precancer produced 95% sensitivity (SE) and 96% specificity (SP) for discriminating normal and human papillomavirus (HPV)-infected tissues from cervical intraepithelial neoplasia (CIN) lesions. For a diagnostic algorithm, 91% SE and 90% SP are achieved for discriminating normal tissue, HPV infected tissue, and low-grade CIN lesions from high-grade CIN lesions. The results demonstrate that the quantitative colposcopic imaging system could provide objective screening and diagnostic information for early detection of cervical cancer. © *2010 Society of Photo-Optical Instrumentation Engineers.* [DOI: 10.1117/1.3365940]

Keywords: acetowhitening; cervical cancer; principal component analysis; support vector machine.

Paper 09404R received Sep. 11, 2009; revised manuscript received Dec. 19, 2009; accepted for publication Jan. 7, 2010; published online Mar. 22, 2010.

1 Introduction

Cervical cancer is the second most common cancer in women worldwide. The major underlying cause of cervical cancer is the infection with certain types of human papillomavirus (HPV). After HPV infection, a small percentage of women will develop cervical intraepithelial neoplasia (CIN), which is graded into three classes (CIN 1, 2, and 3) based on changes in tissue morphology. The majority of cases with mild dysplasia, CIN 1, spontaneously regress to normal, but most cases with more severe lesions, CIN 2 and 3, will progress to invasive cervical cancer. It is therefore important to distinguish CIN 2 and 3 lesions from CIN 1 lesions, HPV-infected tissue, and normal tissue in the clinic to prevent cervical cancer progression. The Pap smear and colposcopy are the primary screening and diagnostic tests for the early detection of neoplastic growth in the cervix. Because the mean sensitivity of Pap smear is[1] lower than 50%, further diagnosis by colposcopy is required to confirm the result of an abnormal Pap smear. In a meta-analysis of the performance of conventional diagnostic colposcopy for distinguishing high-grade CIN and cancerous tissue from the low-grade CIN and non-CIN tissue, the sensitivity was found[2] to be high (64 to 99%) with a mean

of 85%, whereas the specificity was lower (30 to 93%) with a mean of 69%.

The diagnostic information produced by colposcopy is based on the analysis of the acetic-acid-induced whitening or acetowhitening effect in tissue. After applying 3 to 5% acetic acid to the cervix, abnormal cervix tissue turns white in a transient and delayed reaction, while normal epithelium maintains a pink translucent color. A contrast between precancerous lesions and normal tissues is therefore visible. The changes disappear when the acetic acid is completely neutralized, therefore making the effect temporary.[3] Long-term experience has demonstrated that the dynamic changes of acetowhitening, such as the maximum whiteness and duration, are statistically correlated[3,4] with the histological grades of CIN. However, the traditional colposcopy procedure is subjective because the diagnostic accuracy very much depends on the experience of the individual physician. Therefore, an objective diagnostic procedure based on quantitative measurement of the kinetics of the acetowhitening process could substantially improve the diagnostic accuracy in the detection of early cancer lesions.[5–9]

Recently, we reported a new imaging technique that combines 3-D imaging and motion tracking to enable quantitative mapping of acetowhitening kinetics over the cervical surface.[8,9] Briefly, the system consists of a three-CCD color camera, a ring LED illuminator, and a structured laser light

---

*Current address: Beckman Laser Institute and Medical Clinic, University of California, Irvine, 1002 Health Sciences Road, Irvine, California 92612.
†Address all correspondence to: Jianan Y. Qu, Department of Electronic and Computer Engineering, Hong Kong University of Science and Technology, Clear Water Bay Road, Kowloon, Hong Kong China. Tel: 852-2358-8541; Fax: 852-2358-1485; E-mail: eequ@ust.hk

projector that projects a multistriped pattern on the imaged object. With a simple calibration of imaging and projection channels of the imaging system, 3-D coordinates of the laser stripes can be measured for reconstructing the surface topology of the imaged object. The 3-D surfaces measured at different times are used to track the motion of the object. Clinically, the 3-D topology of the cervical surface is reconstructed and the motion of the patient is tracked in 3-D space. The information of motion tracking is then used for the registration of time-sequenced images of the cervix recorded right after the application of acetic acid and continuously throughout the acetowhitening process. The misalignments in the 2-D images of the cervical surface caused by the movement of the patient during the examination are corrected by using the 3-D tracking information so that the dynamic process of the acetowhitening of cervical tissue can be accurately measured to provide the diagnostic information about early development of cervical cancer. Without image registration, the measurement of acetowhitening kinetics using the time-sequenced images would generate false diagnostic information because of the motion of the patient. We found that the kinetics of acetowhitening signals hold the potential to grade the CIN lesions.[9] In this paper, we develop multivariate classification algorithms to distinguish CIN lesions from non-CIN cervical tissues for screening purposes and to distinguish high-grade CIN lesions from low-grade CIN and non-CIN tissues for the diagnostic purposes, respectively. We investigate the potential to achieve objective and computer-aided colposcopy based on the classification of acetowhitening kinetics at the clinical level.

2 Materials and Methods

2.1 Clinical Procedure

The experimental 3-D colposcopic imaging system used for the data acquisition is described in detail elsewhere.[8,9] Briefly, we developed an active stereo vision system to measure the 3-D topology of cervix surface. The system consists of an 8-bit three-CCD color camera, a ring illuminator of 30 blue-light LEDs, and a structured red laser (660-nm) light projector with a 33-stripes pattern. The field of view of the image is about 37×28 mm. The resolution of the imaging system is about 0.05 mm/pixel. To make sure that most of the laser stripes can be projected through the speculum used in colposcopy, the angle between the imaging channel and projection channel was set to about 5 deg and the spacing of the lines of the stripes projected at the cervix tissue is about 0.7 mm. The working distance of the imaging system is about 300 mm.

The image of reflection from cervix and the image of the structured light pattern projected on cervix were captured from blue and red channels of the three-CCD color camera, respectively. The time-sequenced images of the cervix were stored for the analysis of acetowhitening kinetics over the cervix surface. The simultaneously captured images of the structured light pattern on the cervix were used for tracking the motion of the patient.[9] In this paper, one reference image of the cervix was captured before the application of acetic acid. A total of 300 images were captured after the application of acetic acid with a 1-s time interval between two images. Therefore, the acetowhitening kinetics over 300 s was measured. The 3-D surfaces of the cervix measured at different times are used to track the motion and to register the time-sequenced 2-D images. The acetowhitening kinetics, the reflection from cervix as a function of time, could be measured from the intensity of the registered time-sequenced images.

Fifty-seven human subjects originally scheduled for colposcopy and a loop electrosurgical excision procedure (LEEP) were enrolled in the investigation of the imaging technique. To avoid interference from mucus discharge, the cervix was first cleaned with saline before applying 5% acetic acid. A routine colposcopy or LEEP was followed after the 3-D imaging. Tissue biopsies were taken from the subjects' cervices from the sites of the worst suspicious lesions, and from the most possible normal cervical squamous tissues for comparison. The histological analysis of tissue biopsies was performed by experienced pathologists and the histological reports were considered as the ground truth. This study was approved by the Ethical Committee of the Prince of Wales Hospital, the Chinese University of Hong Kong. Consent letters were obtained from all patients enrolled in this study.

2.2 Data Processing of Acetowhitening Kinetics

A variety of multivariate statistical algorithms have been successfully utilized in the diagnosis of tissue.[10–14] In this study, multivariate statistical algorithms based on principal component analysis[15] (PCA) and a support vector machine[16,17] (SVM) were investigated for the diagnosis of CIN lesions based on the classification of the kinetics of the acetowhitening processes. Particularly, PCA was used to reduce the dimension of the acetowhitening kinetics curves for visual separation of the different tissue types, such as CIN lesions and non-CIN tissues. The SVM algorithm was used to classify and grade the CIN lesions because it has been proved as a more effective method to classify multivariate signals when the separating boundaries between data measured from different types of tissues are nonlinear.[13,16,17]

PCA is a method for analyzing the statistical characteristics of multidimensional data.[15] In the application of the PCA method to processing acetowhitening kinetics, the original time-resolved acetowhitening signals were transformed into principal component (PC) scores, which indicated new sets of linear combinations of the informative orthogonal PCs. We first identified the diagnostic informative PCs and calculated the PC scores. The scores of informative PCs are used to illustrate the separation of normal and diseased tissue. The SVM is an effective algorithm for classifying multivariate data. After it was first induced by Vapnik,[16] the SVM has been extensively used in the classification of data, particularly in the processing of biological and medical data.[11–14] We used the nonlinear SVM [radial basis function (RBF) kernel] algorithm to classify tissue based on the correlation between the kinetics of *in vivo* acetowhitening signals and the pathologic states of the tissue sites where the acetowhitening signals were measured. In this work, SVM[light] (version 6.02) was used for the development of classification algorithms.[17] In the learning and testing procedures, each time-resolved acetowhitening kinetics curve was labeled according to the result of histological examination. The kinetics curves of acetowhitening were divided into categories of high-grade CIN, low-grade CIN, HPV, or normal tissue. Optimization of the

SVM algorithms via exhaustive search were performed to maximize the accuracy to distinguish CIN lesions from non-CIN cervical tissues for screening purposes and to distinguish high-grade CIN lesions from low-grade CIN and non-CIN tissues for diagnostic purposes, respectively. Details of the development of an SVM algorithm were described in our previous study.[13]

To evaluate the performance of the diagnostic algorithm, the leave-one-out cross-validation and k-fold cross-validation were used to calculate the sensitivity (SE) and specificity (SP) of the SVM algorithms. In each round of the leave-one-out cross-validation, one acetowhitening kinetics curve was held out from a total of 137 *in vivo* acetowhitening kinetics curves measured from all the cervical tissue samples. The remaining acetowhitening kinetics curves were used as a training set for construction and optimization of the SVM algorithm. The held-out acetowhitening kinetics curve was then classified by the optimized algorithm. This process was repeated until all the acetowhitening kinetics curves in the data set were classified. The criterion for optimizing the algorithms in the training set was to maximize the classification accuracy and the SE in the training set. The final SE and SP of a particular algorithm were calculated based on the classification of the held-out acetowhitening signal in the test set in each round of cross validation. In the k-fold cross-validation, the data set was randomly divided into k subsets. Then k-1 subsets were used for training, and the last subset was used for evaluation. This process was repeated k times, leaving a different subset for evaluation each time. The k cross-validation estimates were averaged to provide the aggregated classification accuracy of the SVM algorithms. The leave-one-out cross-validation is similar to the k-fold cross-validation where the value of k is set to the sample size.

The disadvantage of leave-one-out cross-validation is that the results could be biased because of overtraining of the algorithm.[18,19] The k-fold cross-validation can reduce the bias caused by overtraining and the variance associated with the validation process. The empirical studies[18,19] indicated that the optimal number of folds for k-fold cross-validation is 10. However, because the sample size of normal tissue and CIN 1 lesions in this work were relatively small, the sample number in each subset would be too small if the samples are divided into 10 subsets. We compromised to choose the number of folds as five, as the previously reported studies with relatively small sample volumes.[19,20] To further reduce the bias, we randomly divided the samples in each category into five subsets and performed the fivefold cross-validation. The random division of samples and fivefold cross-validation were repeated by a large number of rounds ($> 10^4$). This helped us to determine the lower boundary of the algorithm performance with the worst subdivision.

A receiver operating characteristics (ROC) curve is used in this study to visualize and to select different classifiers based on their performance.[21] Areas under the ROC curve (AUC) can be used to quantify the performance of the classifier.[18] Moreover, the optimal cutoff points can be determined from the ROC curve to best balance the SE and SP, where the optimal SE and SP are defined[22] as those producing the minimal value for $(1 - SE)^2 + (1 - SP)^2$. In this study, we used this method to evaluate the SE and SP of the ROC curves.

3 Results and Discussion

3.1 *Measurement of Acetowhitening Kinetics in Vivo*

The 3-D colposcopic imaging system was evaluated *in vivo*. A representative result of image registration on a tissue sample without treatment with acetic acid is shown in Fig. 1. A reference image and an unregistered target image captured with a 35-s interval are shown in Figs. 1(a) and 1(b), respectively. The obvious misalignment between the two images was caused by an about 3.0 mm cervix movement of the subject. The registered target image to the reference image is shown in Fig. 1(c). Because there are no reliable landmarks on the cervix surface for quantitative measurement of the accuracy of image registration, we compare the intensity profiles along the direction of movement of the cervix from the reference image, the unregistered target image, and the registered target image. The comparison provides an evaluation on how accurately the target images are registered to the reference image. As shown in Fig. 1(d), the profile measured from unregistered target image along line A-B (blue line) and the line profile measured from the reference image (red line) are not correlated at all because of large motion of cervix. However, the profiles measured along line A-B from the registered target image (green line) and the reference image are highly overlapped with each other, indicating the target images are accurately registered to the reference image. To quantify the registration accuracy, the corresponding profile peaks were picked up and the distance between the corresponding profile peaks were calculated. In Fig. 1(d), the peaks in intensity profile in the reference image (labeled by red open circles) and the corresponding peaks in intensity profiles in the registered images (green open circles) were used for the calculation. The mean distance between the corresponding profile peaks is 0.67 ± 0.82 pixels after image registration, equivalent to a 0.03-mm error for the registration of images shown in Figs. 1(a) and 1(b). The statistical results based on 92 measurements from 23 images of two subjects enrolled in the study with large and small motions show that the mean distance between the corresponding profile peaks is 1.26 ± 0.99 pixels after image registration,[9] equivalent to a 0.06-mm error in the field of view. This demonstrates that the 3-D colposcopic imaging technique can accurately track the patient's motion and register the 2-D images recorded during the examination. More detailed discussions on the tracking technology and the results of image registration were reported in our previous study.[8,9] The acetowhitening kinetics of the tissue sites of interest were measured from the registered images recorded in time sequence over 300 s. In each patient, biopsies were taken from two or three sites of interest for pathological analysis. A total of 137 biopsies were taken from 57 patients enrolled in this study. As shown in Table 1, the pathologists identified four types of tissues from the biopsies, including 12 samples of normal tissue, 66 samples of HPV infected tissue, 15 samples of low-grade lesions (CIN 1), and 44 samples of high-grade lesions (CIN 2 and 3). To investigate the correlations between the acetowhitening kinetics and tissue pathology, we related the acetowhitening kinetics measured from the biopsy sites to the results of their pathologic analysis. We took a video recording when the colposcopist conducted the biopsy from the cervix. The video images showed the precise location of biopsy. We compared the image showing the biopsy site with the images previously cap-
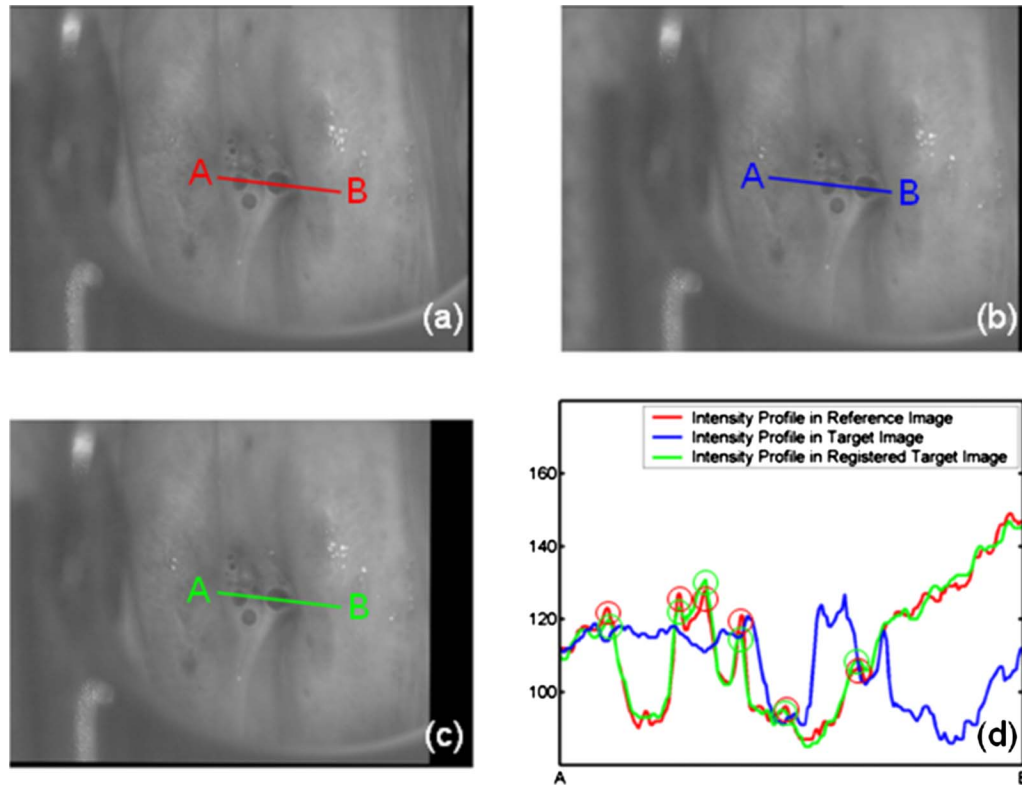
Fig. 1 Representative results of image registration measured from a human subject: (a) reference image; (b) unregistered target image; (c) registered target image; and (d) intensity profiles along *A-B* in (a), (b), and (c).

tured for acetowhitening measurements. We identified the corresponding site in the images for acetowhitening measurements where the biopsy was taken. The difference in locations between the exact biopsy site and the optical measurement site was sufficiently small compared with the CIN lesion size (normally a few millimeters). The statistical results are presented in Fig. 2. As we can see, the kinetics of acetowhitening measured from different types of tissues are distinct.

Note that the representative results in Fig. 2 are slightly different from the results shown in Fig. 6 of the previous study in Ref. 9, though the tendencies in the two figures are the same. There may be a few factors that caused the difference. The kinetics curves of acetowhitening signals vary from patient to patient and even from tissue site to site in the same patient. Only 10 patients were enrolled in the previous clinical pilot study. The results based on such a small sample volume do not produce a high statistical significance and may deviate from the results obtained in this study with a much longer enrolment of human subjects. Furthermore, the results shown in the previous study were based on colposcopy diagnosis and

were not based on pathological analysis, the gold standard of diagnosis, as used in this study. The diagnostic error made by the colposcopist could lead to the corresponding kinetics curves of acetowhitening being labeled with the wrong pathological status.

3.2 Multivariate Statistical Classification

As shown in Fig. 2, tissues in different pathological categories could be roughly separated based on their kinetics curves of

Table 1 Pathological results of biopsies from 57 subjects.

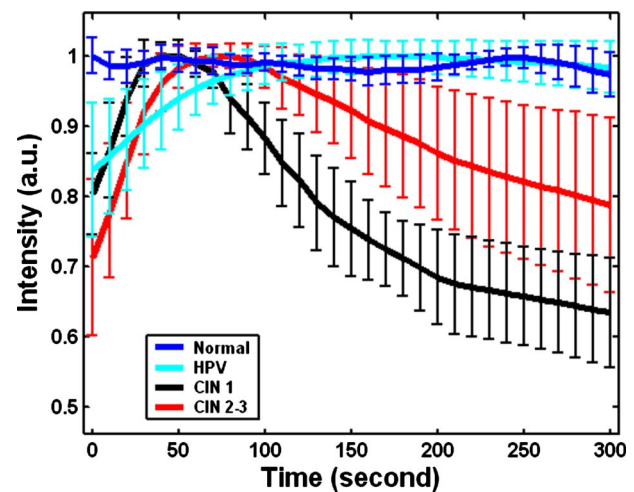|	Normal	HPV	CIN 1	CIN 2 and 3	Total
Subjects	12	36	12	23	—
Number of biopsy	12	66	15	44	137

Fig. 2 Kinetics of acetowhitening for each type of tissues measured from 57 subjects over 300 s after the application of acetic acid.
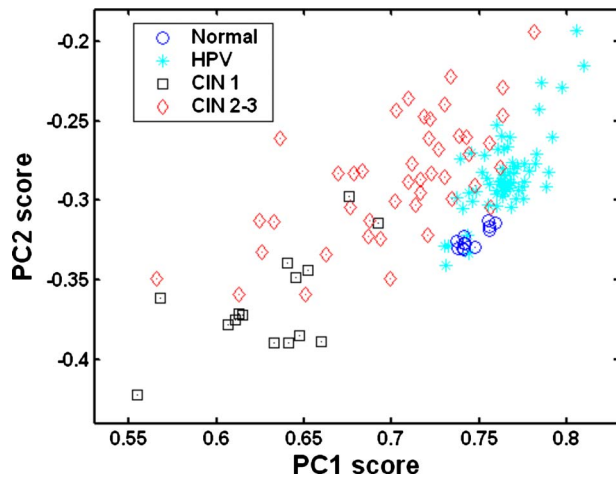
Fig. 3 Scatter plot of PC1 and PC2 scores for normal, HPV, CIN 1, and CIN 2 and 3 tissue samples.

acetowhitening. To create a clear and simple visualization of tissue classification, we used a PCA algorithm to calculate the PCs from the 137 acetowhitening kinetics curves and to identify their diagnostic relevance. In the PC-score-based method, the proportion of variations explained by the PCs determines the number of informative PCs. We found that the first two PCs accounted for 93% of the data variation, while each higher order PC then accounted for less than 4%, suggesting that the higher order PCs were not significant to present the data. This indicates that use of the first two PCs could be adequate to extract significant data variation for diagnosis. The scatter plot of the first two PC scores is shown in Fig. 3. As we can see in the figure, the difference in PC scores between CIN lesions and non-CIN tissues are statistically significant. The p values from a t test are 2.28×10^{-22} and 0.006 for the PC1 and PC2 scores, respectively. Therefore, the classification of samples could be based on the PC1 and PC2 score values. The classification using PC scores also shows that the boundary between different tissue types, especially between high-grade CIN lesions and the rest, are not linear. In this work, a nonlinear SVM method that can effectively classify data with a nonlinear boundary was used to develop algorithms for screening and diagnostic purposes. We compared the difference in performance between the SVM algorithm based on the first two PCs and the algorithm using the whole kinetics curve without a reduction of data dimension.

In the first trial, we used the nonlinear SVM algorithm to classify CIN lesions and non-CIN tissues for the purposes of screening for CIN lesions. In the leave-one-out cross-validation, the optimized parameters of the SVM algorithm developed from the training set were used to classify the held-out acetowhitening kinetics curves. The results of the classifications using the first two PC scores and whole kinetics curve of the acetowhitening signals are summarized in Table 2. With the SVM algorithm, we were able to identify 56 of 59 CIN lesions and 75 of 78 non-CIN tissue samples correctly. Thus, the CIN lesions could be distinguished with an SE of 95% and an SP of 96%. In detail, all of the samples diagnosed as normal tissue and CIN 1 lesions were identified correctly. Three of 66 HPV-infected samples were misdiagnosed, as

Table 2 Classification of acetowhitening kinetics with the algorithms for screening purpose.

Algorithms	SE (%)	SP (%)	Accuracy (%)
2 PC scores + SVM (RBF)	94.9	96.2	95.6
SVM (RBF)	94.9	96.2	95.6

well as 3 of 44 CIN 2 and 3 lesions. Compared to the Pap smear screening method[1] with less than 50% SE, the SVM algorithm can improve the SE to a great extent while maintaining high SP. The results in the table show that the accuracy of the nonlinear SVM algorithm using only two PC scores and the whole acetowhitening signals are identical, demonstrating again that the first two PCs carry the most diagnostic information to separate CIN tissue from non-CIN tissue.

In the second trial, we used the SVM algorithm to classify high-grade CIN lesions (CIN 2 and 3) from low-grade lesions (CIN 1) and non-CIN tissue for diagnostic purposes. The results of the nonlinear SVM classifications using the first two PC scores and the whole acetowhitening signals based on leave-one-out cross-validation are summarized in Table 3. With a nonlinear SVM algorithm based on the first two PCs, we could obtain an SE of 91% and an SP 87% for the separation of CIN 2 and 3 lesions from other tissue types. When using the whole acetowhitening kinetics signals, the nonlinear SVM algorithm could generate a slightly higher accuracy than only using the first two PC scores. The SE and SP are 91 and 90%, respectively. This may be caused by the fact that when projecting the acetowhitening kinetics signals only to the space of the first two PC scores, some information useful for the classification of the high-grade CIN lesions from other types of tissues was lost.

As shown in Fig. 3, it is not possible to discriminate high-grade CIN lesions from other types of tissue with a single linear boundary. However, the nonlinear SVM algorithm can generate a nonlinear boundary in the space of the first two PC scores to differentiate the CIN 2 and 3 lesions from other tissue types. When we compare the algorithm for diagnostic purposes with the accuracy of the algorithm for screening CIN lesions, the performance of diagnostic algorithm is poorer. This was mainly caused by the fact that part of the acetowhitening kinetics curves of CIN 1 lesions were highly overlapped with the acetowhitening kinetics curves measured from CIN 2 and 3 lesions. In addition, there were only 15 CIN 1 lesions out of 137 cases in this study. When the sample size of CIN 1 lesions was small, one or two misclassifications of

Table 3 Classification of acetowhitening kinetics with the algorithms for diagnostic purpose.

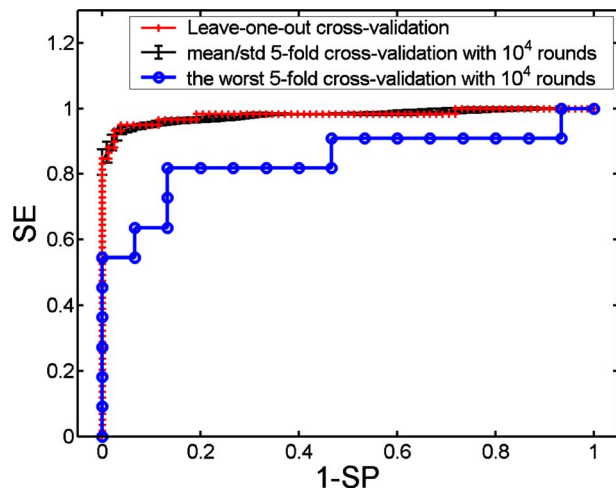| Algorithms	SE (%)	SP (%)	Accuracy (%)
2 PC scores + SVM (RBF)	90.9	87.1	88.3
SVM (RBF)	90.9	90.3	90.5

Fig. 4 ROC curves of leave-one-out and fivefold cross-validations of SVM algorithms for screening purposes.

CIN 1 lesions could reduce the SP significantly. In future work, it is necessary to increase the sample number of CIN 1 lesions to make the classification algorithms more robust.

To reduce the possible bias caused by overtraining in the leave-one-out cross-validation, we evaluated the nonlinear SVM algorithms for screening and diagnostic purposes by using k-fold cross-validation and setting $k=5$ (Refs. 18–20). Compared with the leave-one-out cross-validation, this validation is closer to a clinical condition. To avoid any loss of diagnostic information, we developed the nonlinear SVM algorithms using the whole acetowhitening signals instead of the first two PC scores. As described in Sec. 2, the fivefold cross-validations with random division of samples in each pathological category were repeated over 10^4 rounds. The corresponding mean and the worst ROC curves of diagnostic accuracy for screening and diagnostic purposes were determined and are presented in Figs. 4 and 5, respectively. As shown in Fig. 4, the mean and the worst AUC for fivefold cross-validation of the SVM algorithm for screening purposes
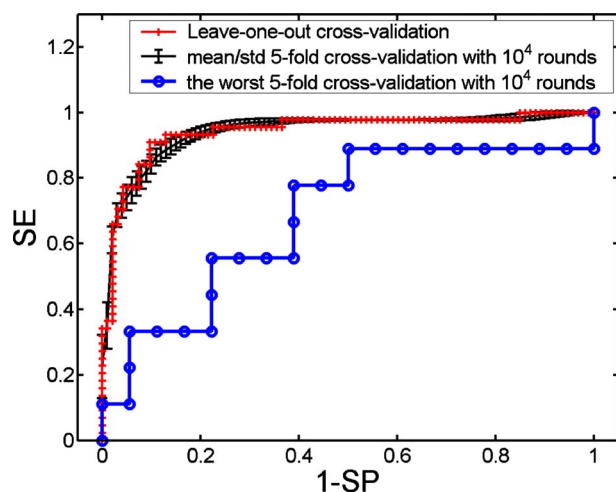

Fig. 5 ROC curves of leave-one-out and fivefold cross-validations of SVM algorithms for diagnostic purposes.

were 0.98 and 0.84, respectively. The evaluations of the algorithm for the diagnostic purposes in Fig. 5 show that the mean and the worst AUC for fivefold cross-validation were 0.94 and 0.69, respectively. After the cut-off points were determined, the balanced SE and SP can be calculated. We found that the worst performances in the fivefold cross-validation still could achieve 82% SE and 87% SP for screening purposes and 78% SE and 61% SP for the diagnostic purposes. These results determined the low boundary of the classification algorithm in the worst situation. However, the averaged performance over 10^4 rounds of fivefold cross-validation could achieve 93% SE and 96% SP for screening purposes and was 89% SE and 89% SP for diagnostic purposes. Note that leave-one-out cross-validation and k-fold cross-validation produced similar results, indicating that based on the data in this study, the disadvantage of overtraining with leave-one-out cross-validation was not being realized. Overall, the classification results from using nonlinear SVM algorithms demonstrate that our colposcopy technique based on 3-D imaging and motion tracking has the potential to make colposcopic diagnosis objective and quantitative. The screening accuracy in discriminating CIN lesions from normal and HPV-infected tissues and the diagnostic accuracy in discriminating high-grade CIN lesions from low-grade CIN lesions, HPV, and normal tissue are significantly higher than the reported SE and SP of conventional methods such as Pap smear and colposcopy.[1,2]

4 Conclusion

We described a novel optical imaging method to make colposcopic diagnosis objective for the early detection of cervical cancer. It provides quantitative diagnostic information and can potentially lead to a development of a fully automated colposcope system. This technology could impact significantly on cervical cancer prevention and management in regions where screening/diagnostic equipment and professional colposcopists are in short supply. In our future work, we plan to integrate the classification algorithms with the 3-D colposcopic imaging of acetowhitening kinetics of cervical tissue and to create an automated instrument for the diagnosis of precancerous lesions in the cervix. Finally, note that this technique can not totally replace conventional colposcopy. In some of cases, the entire transformation zone of the cervix cannot be seen in one view or identified in the field of view, which limits the application of this imaging technique.

References

1. K. Nanda, D. C. McCrory, E. R. Myers, L. A. Bastian, V. Hasselblad, J. D. Hickey, and D. B. Matchar, "Accuracy of the Papanicolaou test in screening for and follow-up of cervical cytologic abnormalities: a systematic review," *Ann. Intern Med.* **132**, 810–819 (2000).
2. M. F. Mitchell, D. Schottenfeld, G. Tortolero-Luna, S. B. Cantor, and R. Richards-Kortum, "Colposcopy for the diagnosis of squamous intraepithelial lesions: a meta-analysis," *Obstet. Gynecol.* **91**, 626–631 (1998).
3. R. Lambert, J. F. Rey, and R. Sankaranarayanan, "Magnification and chromoscopy with the acetic acid test," *Endoscopy* **35**, 437–445 (2003).

4. M. Coppleson, J. C. Dalrymple, and K. H. Atkinson, "Colposcopic differentiation of abnormalities arising in the transformation zone," *Obstet. Gynecol. Clin. North Am.* **20**, 83–110 (1993).

5. C. Balas, A. Dimoka, E. Orfanoudaki, and E. Koumandakis, "In-vivo assessment of acetic acid-cervical tissue interaction using quantitative imaging of backscattered light: its potential use for in-vivo cervical cancer detection grading and mapping," *Proc. SPIE* **3568**, 31–37 (1999).

6. C. Balas, "A novel optical imaging method for the early detection, quantitative grading, and mapping of cancerous and precancerous lesions of cervix," *IEEE Trans. Biomed. Eng.* **48**, 96–104 (2001).

7. B. W. Pogue, H. B. Kaufman, A. Zelenchuk, W. Harper, G. C. Burke, E. E. Burke, and D. M. Harper, "Analysis of acetic acid-induced whitening of high-grade squamous intraepithelial lesions," *J. Biomed. Opt.* **6**, 397–403 (2001).

8. T. T. Wu and J. Y. Qu, "Optical imaging for medical diagnosis based on active stereo vision and motion tracking," *Opt. Express* **15**, 10421–10426 (2007).

9. T. T. Wu, T. Cheung, S. Yim, and J. Y. Qu, "Optical imaging of cervical precancerous lesions based on active stereo vision and motion tracking," *Opt. Express* **16**, 11224–11230 (2008).

10. A. S. Haka, K. E. Shafer-Peltier, M. Fitzmaurice, J. Crowe, R. R. Dasari, and M. S. Feld, "Diagnosing breast cancer by using Raman spectroscopy," *Proc. Natl. Acad. Sci. U.S.A.* **102**, 12371–12376 (2005).

11. S. Ramaswamy, P. Tamayo, R. Rifkin, S. Mukherjee, C. H. Yeang, M. Angelo, C. Ladd, M. Reich, E. Latulippe, J. P. Mesirov, T. Poggio, W. Gerald, M. Loda, E. S. Lander, and T. R. Golub, "Multiclass cancer diagnosis using tumor gene expression signatures," *Proc. Natl. Acad. Sci. U.S.A.* **98**, 15149–15154 (2001).

12. B. Fritz, F. Schubert, G. Wrobel, C. Schwaenen, S. Wessendorf, M. Nessling, C. Korz, R. J. Rieker, K. Montgomery, R. Kucherlapati, G. Mechtersheimer, R. Eils, S. Joos, and P. Lichter, "Microarray-based copy number and expression profiling in dedifferentiated and pleomorphic liposarcoma," *Cancer Res.* **62**, 2993–2998 (2002).

13. W. Lin, X. Yuan, P. Yuen, W. I. Wei, J. Sham, P. Shi, and J. Qu, "Classification of in vivo autofluorescence spectra using support vector machines," *J. Biomed. Opt.* **9**, 180–186 (2004).

14. S. Y. Park, M. Follen, A. Milbourne, H. Rhodes, A. Malpica, N. MacKinnon, C. MacAulay, M. K. Markey, and R. Richards-Kortum, "Automated image analysis of digital colposcopy for the detection of cervical neoplasia," *J. Biomed. Opt.* **13**, 014029 (2008).

15. J. E. Jackson, *A User's Guide to Principal Components*, Wiley, New York (1991).

16. V. Vapnik, *Estimation of Dependencies Based on Empirical Data*, Springer-Verlag, New York (1982).

17. T. Joachims, "Making large-scale SVM learning practical," in *Advances in Kernel Methods—Support Vector Learning*, B. Schölkopf, C. J. C. Burges, and A. J. Smola, Eds., MIT Press, Cambridge (1999).

18. D. L. Olson and D. Delen, *Advanced Data Mining Techniques*, Springer-Verlag, Berlin Heidelberg (2008).

19. L. Breiman and P. Spector, "Submodel selection and evaluation in regression: the X-random case," *Int. Statist. Rev.* **60**, 291–319 (1992).

20. W. Li, S. Venkataraman, U. Gustafsson, J. C. Oyama, D. G. Ferris, and R. W. Lieberman, "Using acetowhite opacity index for detecting cervical intraepithelial neoplasia," *J. Biomed. Opt.* **14**, 014020 (2009).

21. J. A. Swets, "Measuring the accuracy of diagnostic systems," *Science* **240**, 1285–1293 (1988).

22. N. J. Perkins and E. F. Schisterman, "The inconsistency of 'optimal' cutpoints obtained using two criteria based on the receiver operating characteristic curve," *Am. J. Epidemiol.* **163**, 670–675 (2006).